J|A|C|S
ARTICLES
Published on Web 08/10/2002

Role of the Catalytic Triad and Oxyanion Hole in Acetylcholinesterase Catalysis: An ab initio QM/MM Study

Yingkai Zhang,* Jeremy Kua, and J. Andrew McCammon

Contribution from the Howard Hughes Medical Institute, Department of Chemistry and Biochemistry, and Department of Pharmacology, University of California at San Diego, La Jolla, California 92093-0365

Received February 15, 2002. Revised Manuscript Received April 22, 2002

Abstract: The initial step of the acylation reaction catalyzed by acetylcholinesterase (AChE) has been studied by a combined ab initio quantum mechanical/molecular mechanical (QM/MM) approach. The reaction proceeds through the nucleophilic addition of the Ser203 O to the carbonyl C of acetylcholine, and the reaction is facilitated by simultaneous proton transfer from Ser203 to His447. The calculated potential energy barrier at the MP2(6-31+G*) QM/MM level is 10.5 kcal/mol, consistent with the experimental reaction rate. The third residue of the catalytic triad, Glu334, is found to be essential in stabilizing the transition state through electrostatic interactions. The oxyanion hole, formed by peptidic NH groups from Gly121, Gly122, and Ala204, is also found to play an important role in catalysis. Our calculations indicate that, in the AChE−ACh Michaelis complex, only two hydrogen bonds are formed between the carbonyl oxygen of ACh and the peptidic NH groups of Gly121 and Gly122. As the reaction proceeds, the distance between the carbonyl oxygen of ACh and NH group of Ala204 becomes smaller, and the third hydrogen bond is formed both in the transition state and in the tetrahedral intermediate.

1. Introduction

Understanding the structural origin of the catalytic efficiency of enzymes is a fundamental goal and challenge in biological science. An attractive enzyme for such study is acetylcholinesterase (AChE, EC 3.1.1.7), a serine hydrolase responsible for the termination of impulse signaling at cholinergic synapses. It catalyzes the hydrolysis of the neurotransmitter acetylcholine (ACh) with a remarkably high catalytic efficiency, with a second-order reaction rate constant close to the diffusion-controlled limit.[1] The breakdown of ACh into choline and acetic acid by the enzyme acetylcholinesterase (AChE) proceeds in two successive stages, acylation and deacylation, as shown in Figure 1.

Like many other members of the serine hydrolase and serine protease families, the essential catalytic functional unit for acetylcholinesterase is the catalytic triad.[2] In mouse AChE, the catalytic triad consists of Ser203, His447, and Glu334. The mutation of any of these three residues to alanine leads to a decrease in activity of at least 3300-fold.[3] The reaction mechanism in Figure 1 shows that the residues Ser203 and His447 are directly involved in the reaction, serving as nucleophilic attacking group and general acid−base catalytic elements, respectively. However, the catalytic role of the third residue of the catalytic triad, Glu334, remains an open question.[4] In the literature, several different roles for Glu334 have been suggested. The first is that the electrostatic interaction between the carboxylate of Glu334 and the incipient imidazolium cation stabilizes the transition state and the tetrahedral intermediate.[5,6] The second is often called the "charge-relay" mechanism[7,8] where the carboxylate of Glu334 also serves as the general acid−base catalyst, which is involved in the proton transfer between Glu334 and His447. The third and most recent is the "low-barrier hydrogen bond" mechanism,[4,9] wherein the low-barrier hydrogen bond formed between carboxylate of Glu334 and the incipient imidazolium cation of His447 provides a special stabilization energy to lower the reaction barrier.

In addition to the catalytic triad, another important component of the active center in AChE is the oxyanion hole. The X-ray structure of a transition state analogue complex with torpedo AChE[10] revealed that a three-pronged oxyanion hole exists in the active site of AChE, in contrast to the two-pronged oxyanion hole in most serine proteases.[11] The oxyanion hole is formed by peptidic NH groups from Gly118, Gly119, and Ala201,

* Address correspondence to this author. E-mail: yzhang@mccammon.ucsd.edu.

(1) Quinn, D. M. *Chem. Rev.* **1987**, *87*, 955−979.
(2) Dodson, G.; Wlodawer, A. *Trends Biochem. Sci.* **1998**, *23*, 347−352.
(3) Shafferman, A.; Kronman, C.; Flashner, Y.; Leitner, M.; Grosfeld, H.; Ordentlich, A.; Gozes, Y.; Cohen, S.; Ariel, N.; Barak, D.; Harel, M.; Silman, I.; Sussman, J. L.; Velan, B. *J. Biol. Chem.* **1992**, *267*, 17640−17648.
(4) Quinn, D.; Medhekar, R.; Baker, N. Ester hydrolysis. In *Comprehensive Natural Products Chemistry: Enzymes, Enzyme Mechanisms, Proteins, and Aspects of NO Chemistry*; Elsevier Science: Oxford, U.K., 1999.
(5) Warshel, A.; Narayszabo, G.; Sussman, F.; Hwang, J. K. *Biochemistry* **1989**, *28*, 3629−3637.
(6) Fuxreiter, M.; Warshel, A. *J. Am. Chem. Soc.* **1998**, *120*, 183−194.
(7) Blow, D. M.; Birktoft, J. J.; Hartley, B. S. *Nature* **1969**, *221*, 337−340.
(8) Bachovchin, W. W.; Roberts, J. D. *J. Am. Chem. Soc.* **1978**, *100*, 8041−8047.
(9) Massiah, M. A.; Viragh, C.; Reddy, P. M.; Kovach, I. M.; Johnson, J.; Rosenberry, T. L.; Mildvan, A. S. *Biochemistry* **2001**, *40*, 5682−5690.
(10) Harel, M.; Quinn, D. M.; Nair, H. K.; Silman, I.; Sussman, J. L. *J. Am. Chem. Soc.* **1996**, *118*, 2340−2346.
(11) Menard, R.; Storer, A. C. *Biol. Chem. Hoppe-Seyler* **1992**, *373*, 393−400.

10.1021/ja020243m CCC: $22.00

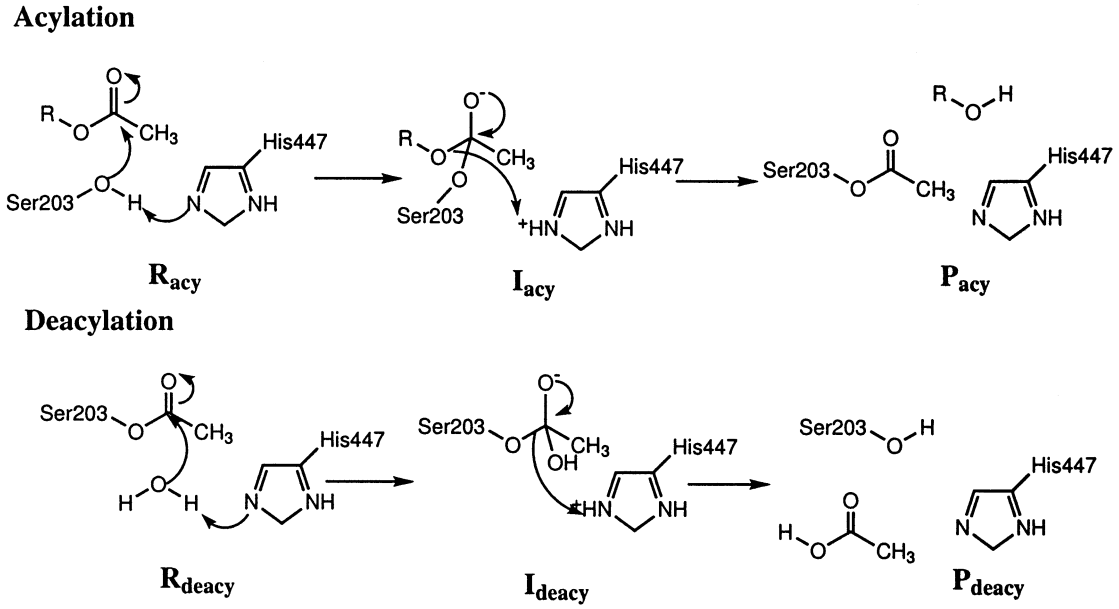

Figure 1. Reaction mechanism of the hydrolysis of ACh catalyzed by AChE.

which form hydrogen bonds with the carbonyl oxygen of the inhibitor, the respective O to N distances being 2.9, 2.9, and 3.2 Å.[10] In mouse AChE, the corresponding residues are Gly121, Gly122, and Ala204. The catalytic role of the oxyanion hole in serine protease is generally established to be in stabilizing high-energy intermediates and the transition state through hydrogen bonding.[5,6,12] The remaining question is whether this is indeed the case for AChE and whether the three hydrogen bonds are always formed during the reaction process.

To elucidate the role of the catalytic triad and the oxyanion hole in acetylcholinesterase catalysis, we have studied the first step of the acylation reaction using the pseudobond ab initio QM/MM approach.[13−15] Our calculations reveal that the catalytic role of Glu334 is to stabilize the transition state and the tetrahedral intermediate through electrostatic interactions. For the oxyanion hole, we find progressive hydrogen-bond formation between the peptidic NH of Ala204 and the carbonyl oxygen of ACh. Our calculated activation barriers are in good agreement with the experimental barrier of 12 kcal/mol.

2. Computational Method and Procedure

Because of the large size of the enzyme system and the fact that the reaction involves the making and breaking of bonds, the study of enzyme reactions remains very challenging for computational methods. High-level quantum mechanical methods can provide the electronic details of chemical reactions but are limited in application to systems of small size. The combined quantum mechanical and molecular mechanical (QM/MM) method extends the realm of quantum mechanical calculations to macromolecules, in which a small active site directly participating in the making and breaking of bonds is treated by quantum mechanical methods while the rest of the enzyme containing a large number of atoms is described by molecular mechanical methods.[16−18]

In the current study, we employed the pseudobond ab initio QM/MM approach,[13−15,19] which has circumvented the major deficiency of the conventional link−atom QM/MM approach by providing a consistent and well-defined ab initio QM/MM potential energy surface. This approach not only allows for the use of ab initio QM/MM methods to determine the reaction path with a realistic enzyme environment, but also allows the enzyme environment to adjust to the movement of the QM atoms in the reactive part during the reaction process. For a detailed comparison between the pseudobond ab initio QM/MM approach and other related approaches, including the link atom,[17,20,21] hybrid orbital,[16,22,23] QM(ai)/MM,[24] and QM-FE,[25,26] please see refs 13−15. For recent reviews on QM/MM methods and their application to enzyme reactions, see refs 27−29.

2.1. Preparation of the Enzyme−Substrate System. The initial structure was chosen from a snapshot of a 10-ns molecular dynamics simulation of the apo-mAChE with explicit water molecules.[30] First, we rotated the ring of His447 into its productive orientation. The apo-enzyme system was then constructed by retaining the whole protein, the sodium cation in the active site, and water molecules within a 24-Å radius of the Ser203 side-chain oxygen. Finally, the active site of the apo-AChE system (within 20 Å of Ser203 side-chain oxygen) was equilibrated by a series of minimizations interspersed by short molecular dynamics simulations.

The structure of the substrate acetylcholine (ACh) was constructed in its fully extended conformation according to early experimental and molecular modeling studies.[10,31] The substrate was then optimized using

(12) Gerlt, J. A.; Gassman, P. G. *Biochemistry* **1993**, *32*, 11934−11952.
(13) Zhang, Y.; Lee, T.; Yang, W. *J. Chem. Phys.* **1999**, *110*, 46−54.
(14) Zhang, Y.; Liu, H.; Yang, W. *J. Chem. Phys.* **2000**, *112*, 3483−3492.
(15) Zhang, Y.; Liu, H.; Yang, W. Ab Initio QM/MM and Free Energy Calculations of Enzyme Reactions. In *Methods for Macromolecular Modeling*; Schlick, T., Ed.; Springer-Verlag: New York, 2001.
(16) Warshel, A.; Levitt, M. *J. Mol. Biol.* **1976**, *103*, 227.
(17) Singh, U. C.; Kollman, P. *J. Comput. Chem.* **1986**, *7*, 718−730.
(18) Field, M. J.; Bash, P. A.; Karplus, M. *J. Comput. Chem.* **1990**, *11*, 700−733.
(19) Liu, H.; Zhang, Y.; Yang, W. *J. Am. Chem. Soc.* **2000**, *122*, 6560−6570.
(20) Maseras, F.; Morokuma, K. *J. Comput. Chem.* **1995**, *16*, 1170.
(21) Eurenius, K. P.; Chatfield, D. C.; Brooks, B. R.; Hodoscek, M. *Int. J. Quantum Chem.* **1996**, *60*, 1189−1200.
(22) Assfeld, X.; Rivail, J.-L. *Chem. Phys. Lett.* **1996**, *263*, 100−106.
(23) Gao, J.; Amara, P.; Alhambra, C.; Field, M. J. *J. Phys. Chem. A* **1998**, *102*, 4714−4721.
(24) Bentzien, J.; Muller, R. P.; Florian, J.; Warshel, A. *J. Phys. Chem. B* **1998**, *102*, 2293−2301.
(25) Chandrasekhar, J.; Smith, S. F.; Jorgensen, W. L. *J. Am. Chem. Soc.* **1985**, *107*, 154−162.
(26) Stanton, R. V.; Perakyla, M.; Bakowies, D.; Kollman, P. A. *J. Am. Chem. Soc.* **1998**, *120*, 3448−3457.
(27) Field, M. J. *J. Comput. Chem.* **2002**, *23*, 48−58.
(28) Gogonea, V.; Suarez, D.; van der Vaart, A.; Merz, K. W. *Curr. Opin. Struct. Biol.* **2001**, *11*, 217−223.
(29) Bruice, T. C.; Kahn, K. *Curr. Opin. Chem. Biol.* **2000**, *4*, 540−544.
(30) Tai, K.; Shen, T. Y.; Borjesson, U.; Philippopoulos, M.; Mccammon, J. A. *Biophys. J.* **2001**, *81*, 715−724.
(31) Sussman, J. L.; Harel, M.; Frolow, F.; Oefner, C.; Goldman, A.; Toker, L.; Silman, I. *Science* **1991**, *253*, 872−879.

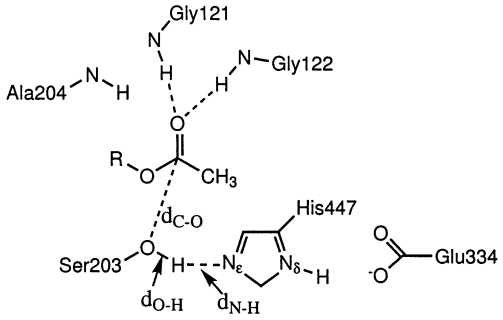

Figure 2. Illustration of the reaction coordinate chosen for the first step of the acylation reaction, which is $d_{O-H}-d_{N-H}-d_{C-O}$.

quantum mechanics at the Hartree−Fock level with the 6-31G* basis set.[32] The ligand charges were obtained from electrostatic potential (ESP) fitted charges[33] from the HF/6-31G* QM calculation.

The AChE−ACh complex was constructed by docking the ligand into the equilibrated apo-AChE system using Autodock 3.0.4.[34] Then, the system was equilibrated with a series of minimizations interspersed by short molecular dynamics simulations. The resulting structure was used as the starting model for the QM/MM study as well as for a 1-ns molecular dynamics simulation. It contained a total of 9859 atoms, including 518 water molecules.

2.2. QM/MM Calculations. For the QM/MM calculations, the prepared enzyme−substrate system was first partitioned into a QM subsystem and an MM subsystem. Because one of our goals was to investigate the catalytic role of Glu334, we used two partition schemes. The first utilized a smaller QM subsystem consisting of the substrate ACh and the side chains of Ser203 and His447, with a total of 44 QM atoms. The second, larger QM subsystem also included the side chain of Glu334, leading to a total of 54 QM atoms. The boundary problem between the QM and MM subsystems was treated using the pseudobond approach.[13]

With this prepared AChE−ACh QM/MM system, an iterative optimization procedure[14] was applied to the QM/MM system with HF/3-21G QM/MM calculations, leading to the optimized structure for the reactant. For the initial step of the acylation reaction, the reaction coordinate chosen was the simultaneous bond formation of the new C−O bond between ACh and Ser203 and the proton-transfer reaction between Ser203 and His447, as illustrated in Figure 2. An iterative restrained minimization was then repeatedly applied to different points along the reaction coordinate, resulting in an optimum path for the reaction in the enzymatic environment and its associated potential energy surface. Stationary points obtained along the minimum-energy paths and Hessian matrices for degrees of freedom involving atoms in the QM subsystem were calculated, leading to the determination of the corresponding vibrational frequencies.[15] The energy maximum on the path with one and only one imaginary frequency is the transition state, whereas the energy minimum along the path with no imaginary frequencies is characterized as the reactant or the intermediate. For the reactant, transition state, and tetrahedral intermediate, we further carried out single-point higher-level (MP2 and B3LYP) QM/MM calculations with a larger 6-31+G* basis set.

2.3. Other Computational Details. The calculations were carried out using modified versions of the Gaussian 98[35] and TINKER programs.[36] For the QM subsystem, criteria used for geometry optimizations follow Gaussian 98 defaults. For the MM subsystem, the convergence criterion used is that the root-mean-square (RMS) energy gradient be less than 0.1 kcal mol^{-1} $Å^{-1}$. In the MM minimizations, only atoms within 20 Å of the oxygen of Ser203 were allowed to move. No cutoff for nonbonded interactions was used in the QM/MM calculations and the MM minimizations. Throughout the QM/MM calculations, pseudobonds were treated with the 3-21G basis set and its corresponding effective-core potential parameters.[13]

We also performed a 1-ns molecular dynamics simulation for the AChE−ACh system. In the simulation, only atoms within 20 Å of the oxygen of Ser203 were allowed to move. The twin-range cutoff method was used to treat the nonbonded interactions,[37] with a long-range cutoff of 12 Å and a short-range cutoff of 8 Å. The nonbonded pair list was updated every 20 steps. The time step used was 2 fs. Bond lengths involving hydrogen atoms were constrained using SHAKE.[38] The temperature of the simulations was maintained at 300 K using the weak coupling method with a coupling time of 0.1 ps.[39] Snapshots of the AChE−ACh system were saved every picosecond, and a total of 1000 snapshots were saved.

The MM force fields used in the present study are the AMBER 95 all-atom force field for the protein[40,41] and the TIP3P model for water.[42]

3. Results and Discussions

The calculated minimum-energy paths are shown in Figure 3, and the calculated potential energy results for the first step of the acylation reaction are presented in Table 1. We can see that the calculations on both small and large QM subsystems are consistent with each other. The determined minimum-energy paths are very smooth as the geometry changes along the reaction coordinate. The reaction proceeds from the reactant to the tetrahedral transition state and then to the high-energy tetrahedral intermediate. The calculated potential energy barrier for MP2(6-31+G*) (12.6 kcal/mol for the small QM subsystem, 10.5 kcal/mol for the large QM subsystem) is consistent with the activation barrier of ∼12 kcal/mol estimated from the experimental value of k_{cat} by simple transition state theory.[1,6]

We also investigated changes in the hydrogen bonds formed between the carbonyl oxygen of ACh and the peptidic NH groups of the three-pronged oxyanion hole (Gly121, Gly122, Ala204). The changes in N−O distances along the reaction coordinate are shown in Figure 4. In the AChE−ACh reactant complex, only two hydrogen bonds are formed between the carbonyl oxygen of ACh and the NH groups of Gly121 and Gly122, with N−O distances of 2.84 and 2.89 Å, respectively.

(32) Hehre, W.; Radom, L.; Schleyer, P.; Pople, J. *Ab Initio Molecular Orbital Theory*; John Wiley & Sons: New York, 1986.
(33) Besler, B. H.; Merz, K. M., Jr.; Kollman, P. A. *J. Comput. Chem.* **1990**, *11*, 431−439.
(34) Morris, G. M.; Goodsell, D. S.; Halliday, R. S.; Huey, R.; Hart, W. E.; Belew, R. K.; Olson, A. J. *J. Comput. Chem.* **1998**, *19*, 1639−1662.
(35) Frisch, M. J.; Trucks, G. W.; Schlegel, H. B.; Scuseria, G. E.; Robb, M. A.; Cheeseman, J. R.; Zakrzewski, V. G.; Montgomery, J. A., Jr.; Stratmann, R. E.; Burant, J. C.; Dapprich, S.; Millam, J. M.; Daniels, A. D.; Kudin, K. N.; Strain, M. C.; Farkas, O.; Tomasi, J.; Barone, V.; Cossi, M.; Cammi, R.; Mennucci, B.; Pomelli, C.; Adamo, C.; Clifford, S.; Ochterski, J.; Petersson, G. A.; Ayala, P. Y.; Cui, Q.; Morokuma, K.; Malick, D. K.; Rabuck, A. D.; Raghavachari, K.; Foresman, J. B.; Cioslowski, J.; Ortiz, J. V.; Stefanov, B. B.; Liu, G.; Liashenko, A.; Piskorz, P.; Komaromi, I.; Gomperts, R.; Martin, R. L.; Fox, D. J.; Keith, T.; Al-Laham, M. A.; Peng, C. Y.; Nanayakkara, A.; Gonzalez, C.; Challacombe, M.; Gill, P. M. W.; Johnson, B. G.; Chen, W.; Wong, M. W.; Andres, J. L.; Head-Gordon, M.; Replogle, E. S.; Pople, J. A. *Gaussian 98*, revision A.5; Gaussian, Inc.: Pittsburgh, PA, 1998.
(36) Ponder, J. W. *TINKER, Software Tools for Molecular Design*, version 3.6; Department of Biochemistry & Molecular Biophysics, Washington University School of Medicine, St. Louis, MO. The most updated version for the TINKER program can be obtained from J. W. Ponder's World Wide Web site at http://dasher.wustl.edu/tinker (Feb 1998).
(37) van Gunsteren, W.; Berendsen, H.; Colonna, F.; Perahia, D.; Hollenberg, J.; Lellouch, D. *J. Comput. Chem.* **1984**, *5*, 272−279.
(38) Ryckaert, J.-P.; Ciccotti, G.; Berendsen, H. J. C. *J. Comput. Phys.* **1977**, *23*, 327−341.
(39) Berendsen, H. J. C.; Postma, J. P. M.; van Gunsteren, W. F.; DiNola, A.; Haak, J. R. *J. Chem. Phys.* **1984**, *81*, 684−3690.
(40) Cornell, W. D.; Cieplak, P.; Bayly, C. I.; Gould, I. R.; Merz, K. M.; Ferguson, D. M.; Spellmeyer, D. C.; Fox, T.; Caldwell, J. W.; Kollman, P. A. *J. Am. Chem. Soc.* **1995**, *117*, 5179−5197.
(41) Fox, T.; Scanlan, T. S.; Kollman, P. A. *J. Am. Chem. Soc.* **1997**, *119*, 11571−11577.
(42) Jorgensen, W. L.; Chandrasekhar, J.; Madura, J.; Impey, R. W.; Klein, M. L. *J. Chem. Phys.* **1983**, *79*, 926−933.

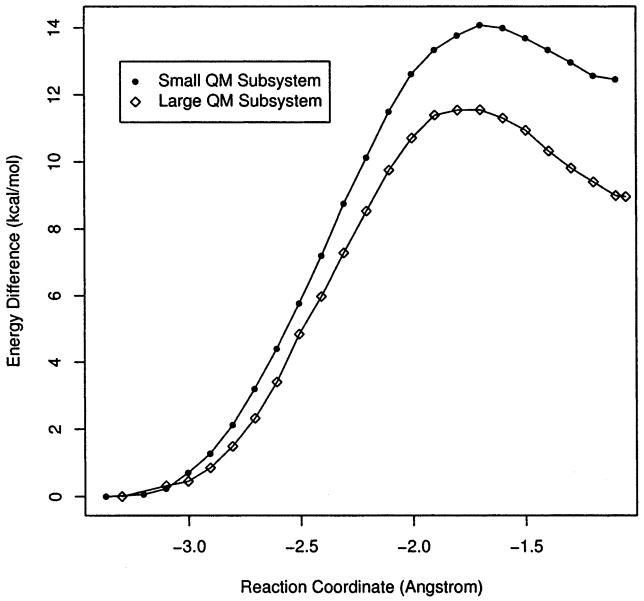

Figure 3. Determined minimum-energy path along the reaction coordinate for the first step of the acylation reaction. From left to right, the reaction proceeds from the reactant to the tetrahedral intermediate through a tetrahedral transition state.

Table 1. Calculated Total QM/MM Potential Energy Difference for the First Step of the Acylation Reaction[a]

	MP2(6-31+G*)/MM	B3LYP(6-31+G*)/MM	HF(3-21G)/MM
	small QM subsystem		
reactant	0.0	0.0	0.0
transition state	12.6	15.8	14.0
intermediate	11.1	15.5	12.5
	large QM subsystem		
reactant	0.0	0.0	0.0
transition state	10.5	13.4	11.6
intermediate	8.4	12.6	9.0

[a] Geometries calculated at the HF/3-21G QM/MM level.

As the reaction proceeds, the distance between the carbonyl oxygen of ACh and the NH group of Ala204 becomes smaller as it forms a weak hydrogen bond both in the transition state and in the tetrahedral intermediate, with the O−N distance changing from 3.59 Å in the reactant complex to 3.15 Å in the tetrahedral intermediate. The N−O distance in the transition state is 3.19 Å. These results are consistent with experimental results on a transition state analogue complex with torpedo AChE,[10] which has N−O distances of 2.9, 2.9, and 3.2 Å to the NH groups of Gly118, Gly119, and Ala201, respectively. It is also consistent with our molecular dynamics simulation results. Throughout the 1-ns molecular dynamics simulation of the AChE−ACh system, we find that only two hydrogen bonds are formed with Gly121 and Gly122, with average N−O distances of 3.01 (±0.18) and 2.92 (±0.13) Å respectively. Ala204 does not form a hydrogen bond with ACh in the simulation, with the average O−N distance being 3.92 (±0.45) Å.

As to the catalytic role of Glu334 for this first step of the acylation reaction, we found that the proton transfer between His447 and Glu334 destabilizes the tetrahedral intermediate, as shown in Figure 5. This indicates that the catalytic role of Glu334 for this first step of the acylation is not likely to proceed through the charge-relay mechanism. In the QM/MM calculation

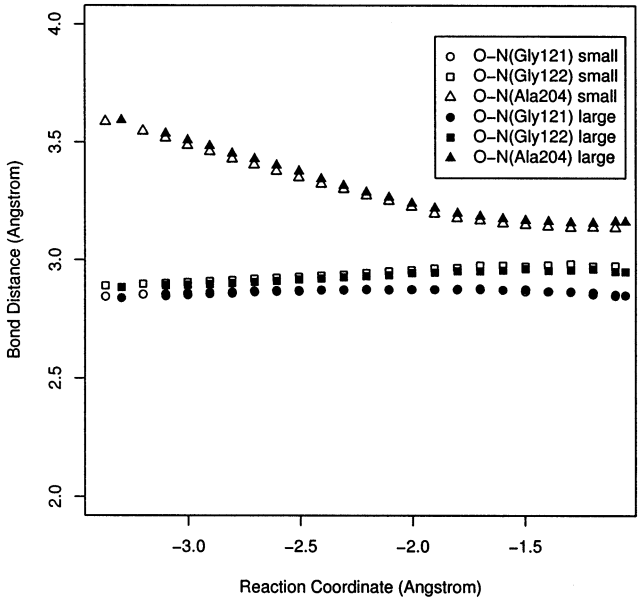

Figure 4. Calculated N−O distances between the carbonyl oxygen of ACh and the NH groups of the oxyanion hole (Gly121, Gly122, Ala204) along the reaction coordinate for the first step of the acylation reaction. Solid symbols are results with the large QM subsystem; open symbols are results with the small QM subsystem.

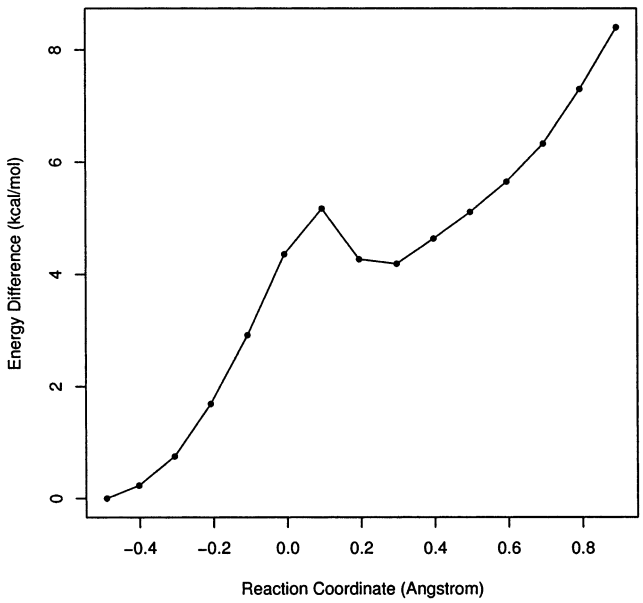

Figure 5. Calculated minimum-energy path for the proton transfer between Glu334 and His447 at the acylation tetrahedral intermediate for the large QM subsystem. The left-hand side of the reaction coordinate is the calculated tetrahedral intermediate state. From left to right, the proton transfers from a ring nitrogen of His447 to the carboxyl oxygen of Glu-334. The reaction coordinate is $R_{N-H}-R_{O-H}$.

with the large QM subsystem, Glu334 is treated quantum mechanically, whereas in the calculation with the small QM subsystem, Glu334 is treated molecular mechanically. In the latter case, the interaction between Glu334 and the QM subsystem is mainly through classical electrostatic interactions. From Table 1, we can see that treating Glu334 quantum mechanically versus classically (i.e., excluding Glu334 from the QM subsystem) decreases the reaction energy barrier by only ∼2 kcal/mol, which can be rationalized by polarization effects. The classical electrostatic contribution of Glu334 to the lowering

Table 2. Residues with Significant Contributions to the Transition State Stabilization or Destabilization[a] According to MP2(6-31+G*)/MM Calculations[b]

residue	VDW	ELE	VDW + ELE
	small QM subsystem		
Asp74	0.0	2.9	2.9
Gly120	−0.2	−2.0	−2.2
Gly121	−0.3	−4.0	−4.3
Gly122	−0.5	−2.6	−3.1
Glu202	−0.1	8.4	8.3
Ala204	−0.4	−4.0	−4.4
Glu334	0.2	−11.5	−11.3
Asp404	0.0	−2.0	−2.0
Pro446	0.2	1.8	2.0
MM total	0.5	−9.7	−9.2
	large QM subsystem		
Asp74	0.0	2.8	2.8
Gly120	−0.1	−1.9	−2.0
Gly121	−0.4	−3.9	−4.3
Gly122	−0.4	−2.8	−3.2
Glu202	−0.1	7.4	7.3
Ala204	−0.4	−3.6	−4.0
Asp404	0.0	−2.0	−2.0
Pro446	0.2	1.9	2.1
MM total	0.5	2.0	2.5

[a] Absolute value larger than 2 kcal/mol. [b] VDW refers to the van der Waals interaction energy. ELE refers to the electrostatic interaction energy. MM total refers to the interaction between the MM and QM subsystems. The small QM subsystem contains ACh, Ser203, and His447. The large QM subsystem contains ACh, Ser203, His447, and Glu334. Energy units are kcal/mol.

of the transition state is about −11.5 kcal/mol as shown in Table 2. Although the value −11.5 kcal/mol is a qualitative and not a quantitative indicator, as explained below, it does suggest that the classical electrostatic interaction of Glu334 is essential for catalysis.

Proton NMR data from human AChE complexed with a transition state analogue inhibitor[9] indicated that a short hydrogen bond (2.62−2.63 Å) is formed between Glu and His of the catalytic triad. This short hydrogen bond was interpreted as a strong hydrogen bond, and it was suggested to partially account for the high catalytic power of AChE catalysis. In our AChE simulation, the calculated Glu−His hydrogen-bond length was 2.63 Å in the transition state, in agreement with the observed NMR data. Our calculations however, indicate that this short hydrogen bond is not a low-barrier hydrogen bond. There is no need to invoke the controversial low-barrier hydrogen bond (or "short, strong hydrogen bond") hypothesis[12,43−48] in AChE, as the electrostatic interaction can well account for the role of Glu334 in catalysis.

To understand the role of each residue toward catalysis, we have analyzed the energy contribution by individual residues as the reaction proceeds from reactant to transition state. The structures and charges of the transition state and the reactant were determined with HF(3-21G)/MP2(6-31+G*) QM/MM calculations. The electrostatic and van der Waals interaction energies between the given residue and the QM subsystem were calculated classically for the transition state and reactant, respectively. The difference between the interaction energies of the reactant and the transition state tells us the contribution to the reaction barrier. The results are shown in Table 2. Negative values indicate that the residue lowers the reaction barrier, whereas positive values indicates the opposite. Because the effects of conformational change and dielectric screening are absent in our analysis and original ab initio QM/MM calculations were performed variationally, we use these values only as a qualitative indicator, not as a quantitative prediction.

From Table 2, we can see that the results for the small QM subsystem and large QM subsystem are consistent with each other. The values in Table 2 refer to the classical interaction *between* the MM and QM subsystems. For the large QM subsystem, Glu334 is treated quantum mechanically and so is not included in the table. The results indicate that Glu334 plays a crucial role in stabilizing the first transition state through electrostatic interactions. The oxyanion hole (Gly121, Gly122, Ala204) also plays an important role in stabilizing the transition state. In addition, Gly120 is found to stabilize the transition state because of the proximity of its backbone to the substrate, consistent with mutation results,[49] whereby the mutation of Gly120, Gly121, or Gly122 to alanine leads to an approximate 100-fold decrease of the bimolecular rate constant for acetylcholine hydrolysis.

An interesting finding is that Glu202 destabilizes the transition state through electrostatic interactions. The main destabilization factor is the electrostatic interaction between Glu202 and ACh due to the decreasing positive charge on the ACh substrate as the reaction proceeds from reactant to transition state. This destabilizing factor outweighs the increasingly favorable interaction between Glu202 and His447 as the Ser203 proton is transferred. Empirical valence-bond calculations on the AChE acylation[6] and deacylation[50] reaction steps have also raised doubts concerning the transition state stabilizing role of Glu202 (199). An early theoretical study[51] suggested that Glu202(199) stabilizes the transition state of acylation through the interaction between Glu202(199) and His447(440); however, the study did not include the enzyme environment, and it modeled ACh as a simple methyl ester without the quaternary ammonium tail group. (The sequence numbers that follow the amino acid abbreviations are those of mammalian AChE, and the numbers in parentheses are those of *Torpedo california* AChE.) The experimental mutation studies[52] showed that the mutation of Glu202(199) to Gln leads to only a 4-fold decrease in k_{cat}, while it increases K_M more than 10-fold. It was also found that the mutation of Glu202 to neutral (Ala, Gln) or acidic (Asp) residues has comparable effects on catalysis for both cationic and neutral substrates.[53] Shafferman et al.[53] proposed that Glu202 might be important for maintaining the "functional architecture" of the active site; however, the comparison of the Glu202Gln mutant structure with the wild-type structure[54] did not provide

(43) Cleland, W. W.; Kreevoy, M. M. *Science* **1994**, *264*, 1887−1990.
(44) Frey, P. A.; Whitt, S.; Tobin, J. *Science* **1994**, *264*, 1927−1930.
(45) Warshel, A.; Papazyan, A.; Kollman, P. A. *Science* **1995**, *269*, 102−104.
(46) Guthrie, J. P. *Chem. Biol.* **1996**, *3*, 163−170.
(47) Ash, E. L.; Sudmeier, J. L.; De Fabo, E. C.; Bachovchin, W. W. *Science* **1997**, *278*, 1128−1132.
(48) Perrin, C. L.; Nielson, J. B. *Annu. Rev. Phys. Chem.* **1997**, *48*, 511−544.
(49) Ordentlich, A.; Barak, D.; Kronman, C.; Ariel, N.; Segall, Y.; Velan, B.; Shafferman, A. *J. Biol. Chem.* **1998**, *273*, 19509−19517.
(50) Vagedes, P.; Rabenstein, B.; Aqvist, J.; Marelius, J.; Knapp, E. W. *J. Am. Chem. Soc.* **2000**, *122*, 12254−12262.
(51) Wlodek, S. T.; Antosiewicz, J.; Briggs, J. M. *J. Am. Chem. Soc.* **1997**, *119*, 8159−8165.
(52) Radic, Z.; Gibney, G.; Kawamoto, S.; MacPhee-Quigley, K.; Bongiorno, C.; Taylor, P. *Biochemistry* **1992**, *31*, 9760−9767.
(53) Shafferman, A.; Ordentlich, A.; Barak, D.; Kronman, C.; Ariel, N.; Velan, B. Contribution of the active center functional architecture to AChE reactivity toward substrates and inhibitors. In *Structure and Function of Cholinesterases and Related Proteins*; Plenum Press: New York, 1998.
(54) Kryger, G.; Harel, M.; Giles, K.; Toker, L.; Velan, B.; Lazar, A.; Kronman, C.; Barak, D.; Ariel, N.; Shafferman, A.; Silman, I.; Sussman, J. L. *Acta Crystallogr. D: Biol. Crystallogr.* **2000**, *56*, 1385−1394.

direct support for this suggestion. Other interesting experimental results associated with the Glu202(199) mutation are that it greatly affects reversible substrate inhibition[52] and it also affects the dependency of k_{cat} on the ionic strength.[55]

In light of the experimental results and our current computational results, we believe that the role of Glu202 in AChE catalysis might be quite complex. We propose the following possible roles of Glu202 in the AChE catalysis: (1) Glu202 might be important for substrate binding, which affects both the binding strength and the binding orientation of the substrate. The effect on the orientation of the substrate might have an important effect on the reaction barrier. (2) The destabilizing effect of Glu202 toward the transition state structure interplays with the stabilizing effects from Glu334, the oxyanion hole, and Gly120. Mutation of Glu202 reduces the destabilizing effect of Glu202 on the transition state structure, but it might also reduce the stabilizing effects of the oxyanion hole, Gly120, and other residues. (3) A cation other than the ligand might be able to bind near Glu202, especially when the ionic strength is high. According to our results, the binding of a cation near Glu202 is likely to lower the acylation reaction barrier. This might explain the experimental fact[55] that in the wild-type enzyme, k_{cat} increases with ionic strength whereas k_{cat} is independent of ionic strength for the Glu202Gln mutant. (4) Glu202 might play an important role in the deacylation step. The above suggestions need to be verified or ruled out in future theoretical and experimental studies.

4. Conclusion

Our ab initio QM/MM calculations confirm that the acylation reaction proceeds via nucleophilic addition of the Ser203 O to the carbonyl C of ACh. This reaction is facilitated by simultaneous proton transfer from Ser203 to His447, leading to the tetrahedral intermediate. The calculated reaction energy barrier for this first step of the acylation is in good agreement with the experimental value of 12 kcal/mol.

As to the catalytic role of the third residue of the catalytic triad, Glu334, our calculations confirm that it is essential in stabilizing the transition state through electrostatic interactions. This conclusion is similar to that reached by effective valence-bond calculations.[6] At the same time, our calculations do not support the charge-relay mechanism or the low-barrier hydrogen bond mechanism.

The peptidic NH groups from Gly121, Gly122, and Ala204 are confirmed to form a three-pronged oxyanion hole in the active site of mAChE. However, from both ab initio QM/MM studies and molecular dynamics simulations, we find that only two hydrogen bonds are formed between the carbonyl oxygen of ACh and the peptidic NH groups of Gly121 and Gly122 in the AChE−ACh reactant complex. As the reaction proceeds from the reactant to the transition state, the distance between the carbonyl oxygen of ACh and the NH group of Ala204 becomes smaller, and the third hydrogen bond is formed in both the transition state and the tetrahedral intermediate. We find that the interaction between the oxyanion hole and the reactive part of the enzyme system stabilizes the transition state. We also find that the role of Glu202 in AChE catalysis is quite complex. It does not stabilize the transition state of the acylation step through electrostatic interactions. This warrants additional theoretical and experimental studies.

Acknowledgment. We are grateful for helpful discussions with Prof. Palmer Taylor, Mr. Kaihsu Tai, and Dr. Richard Henchman. This work has been supported in part by grants from the NSF and NIH. Additional support has been provided by NBCR and the W. M. Keck Foundation.

JA020243M

(55) Radic, Z.; Kirchhoff, P. D.; Quinn, D. M.; McCammon, J. A.; Taylor, P. *J. Biol. Chem.* **1997**, *272*, 23265−23277.